

# AN IMPLEMENTATION OF THE DEUTSCH-JOZSA ALGORITHM ON A THREE-QUBIT NMR QUANTUM COMPUTER

**Noah Linden**<sup>1</sup>

Isaac Newton Institute for Mathematical Sciences, 20 Clarkson Road, Cambridge, CB3  
0EH, UK

and

Department of Applied Mathematics and Theoretical Physics, Silver Street, Cambridge  
CB3 9EW, UK

**Hervé Barjat**<sup>2</sup> and **Ray Freeman**<sup>3</sup>

Department of Chemistry, Lensfield Rd, Cambridge CB2 1EW, UK

## ABSTRACT

A new approach to the implementation of a quantum computer by high-resolution nuclear magnetic resonance (NMR) is described. The key feature is that two or more line-selective radio-frequency pulses are applied simultaneously. A three-qubit quantum computer has been investigated using the 400 MHz NMR spectrum of the three coupled protons in 2,3-dibromopropanoic acid. It has been employed to implement the Deutsch-Jozsa algorithm for distinguishing between constant and balanced functions. The extension to systems containing more coupled spins is straightforward and does not require a more protracted experiment.

---

<sup>1</sup>n1101@newton.cam.ac.uk

<sup>2</sup>hb232@cus.cam.ac.uk

<sup>3</sup>rf110@cus.cam.ac.uk; author to whom correspondence should be addressed.

# 1 Introduction

While there has long been theoretical interest in the notion of a quantum computer, it was the series of recent results leading to the remarkable algorithm of Shor [1] for finding prime factors in polynomial time which led to the recent explosion of interest in the subject. These theoretical results have led many groups to try to realise a quantum computer experimentally. Nuclear magnetic resonance offers a particularly attractive implementation of quantum computers because nuclear spins are relatively weakly coupled to the environment, and there is a long history of development of experimental techniques for manipulating the spins using radio frequency pulses.

A number of groups have already demonstrated the use of NMR computers [2, 3, 4, 5, 6, 7, 8, 9, 10]. One of the key challenges is to try to increase the size of the system used. Previous work on implementing quantum algorithms has focussed on two algorithms in particular, the Deutsch-Jozsa [11] algorithm for distinguishing between balanced and constant functions and Grover's algorithm [12] for searching a database. Previous work on both of these algorithms has used NMR computers with two qubits. In this paper we take the study further by implementing the Deutsch-Jozsa algorithm for a system of three qubits. A particularly notable feature of the experiments we describe is the use of *simultaneous line-selective pulses* to implement the key stage of the algorithm, quantum gates which are closely related to the controlled-controlled-not gate.

The Deutsch-Jozsa algorithm which we will implement is to distinguish between two classes of two-bit binary functions:

$$f : \{0, 1\} \times \{0, 1\} \mapsto \{0, 1\}. \quad (1)$$

The two classes are the *constant* functions, in which all input values get mapped to the same output value, and the *balanced* functions in which exactly two of the inputs get mapped to 0. The eight balanced or constant functions are given in Table 1.

The point of the Deutsch-Jozsa algorithm is that it is possible to decide whether a function is constant or balanced with only one evaluation of the function  $f$ .

The theoretical steps of the quantum algorithm are as follows:

[1] **Preparation:** Prepare the system in the (pure) state  $\psi_1 = |0\rangle|0\rangle|0\rangle$ .

[2] **Excitation:** Perform rotations of the spins about the  $y$ -axis so that the state becomes

$\psi_2 = (|0\rangle + |1\rangle)(|0\rangle + |1\rangle)(|0\rangle - |1\rangle)$ .

**[3] Evaluation:** This is done by implementing the unitary transformation

$$|i\rangle|j\rangle|k\rangle \mapsto |i\rangle|j\rangle|k + f(i, j)\rangle, \quad (2)$$

where the addition is performed modulo two. The three qubits are now in the state

$$\sum_{i,j=1}^2 (-1)^{f(i,j)} |i\rangle|j\rangle(|0\rangle - |1\rangle). \quad (3)$$

For example in the case of the function  $f_4$ , the state is  $\psi_3 = -(|0\rangle - |1\rangle)(|0\rangle + |1\rangle)(|0\rangle - |1\rangle)$ .

The function  $f_4$  is implemented by applying the unitary operator

$$U_4 = \begin{pmatrix} 0 & 1 & 0 & 0 & 0 & 0 & 0 & 0 \\ 1 & 0 & 0 & 0 & 0 & 0 & 0 & 0 \\ 0 & 0 & 0 & 1 & 0 & 0 & 0 & 0 \\ 0 & 0 & 1 & 0 & 0 & 0 & 0 & 0 \\ 0 & 0 & 0 & 0 & 1 & 0 & 0 & 0 \\ 0 & 0 & 0 & 0 & 0 & 1 & 0 & 0 \\ 0 & 0 & 0 & 0 & 0 & 0 & 1 & 0 \\ 0 & 0 & 0 & 0 & 0 & 0 & 0 & 1 \end{pmatrix} \quad (4)$$

to the state. We note that this may be written as

$$U_4 = \begin{pmatrix} 2\sigma_x & 0 & 0 & 0 \\ 0 & 2\sigma_x & 0 & 0 \\ 0 & 0 & E & 0 \\ 0 & 0 & 0 & E \end{pmatrix} \quad (5)$$

where  $\sigma_x$  is the Pauli matrix normalized so that  $\text{tr}(\sigma_x^2) = \frac{1}{2}$  and  $E$  is the  $2 \times 2$  identity matrix. For convenience we will denote such block diagonal matrices by the symbol  $\Delta$ , so that we write

$$U_4 = \Delta(2\sigma_x, 2\sigma_x, E, E). \quad (6)$$

The complete list of unitary operators corresponding to the eight balanced or constant functions is given in Table 2.

**[4] Observation:** By rotating back by the inverse of the transformation applied in the excitation stage, it may be noted that the outputs from the unitary operators corresponding

to the constant functions  $f_1$  and  $f_2$  have a component proportional to  $|0\rangle|0\rangle|0\rangle$ , whereas the outputs from the balanced functions  $f_3 \dots f_8$  are orthogonal to this vector so that the constant and balanced functions may be distinguished from each other with probability one by a von Neumann measurement.

The ensemble nature of an NMR quantum computer means that the implementation of the algorithm differs somewhat from the theoretical version. In particular the preparation stage differs since the states of the system are not pure and the observation stage does not use a von Neumann measurement but measures the amplitudes of spectral lines. Nonetheless the key goal of the algorithm remains to determine whether the unitary operator which acts on the system in the third step corresponds to a constant or balanced function.

One way to proceed would be to follow [3] and produce a pseudo-pure state in the preparation stage. In terms of product operators, the state corresponding to the pure state  $\psi_1 = |0\rangle|0\rangle|0\rangle$  is written

$$\rho(\psi_1) = \mathbf{I}_z + \mathbf{S}_z + \mathbf{R}_z + 2\mathbf{I}_z\mathbf{S}_z + 2\mathbf{I}_z\mathbf{R}_z + 2\mathbf{S}_z\mathbf{R}_z + 4\mathbf{I}_z\mathbf{S}_z\mathbf{R}_z. \quad (7)$$

$\mathbf{I}$  refers to the first spin,  $\mathbf{S}$ , the second and  $\mathbf{R}$ , the third.

This state is excited to  $\rho(\psi_2) = \mathbf{I}_x + \mathbf{S}_x - \mathbf{R}_x + 2\mathbf{I}_x\mathbf{S}_x - 2\mathbf{I}_x\mathbf{R}_x - 2\mathbf{S}_x\mathbf{R}_x - 4\mathbf{I}_x\mathbf{S}_x\mathbf{R}_x$  in stage [2].

In the evaluation stage, the state to which the spins evolve depends on which function is being implemented. For example the unitary operator corresponding to  $f_4$  produces  $\rho(\psi_3) = -\mathbf{I}_x + \mathbf{S}_x - \mathbf{R}_x - 2\mathbf{I}_x\mathbf{S}_x + 2\mathbf{I}_x\mathbf{R}_x - 2\mathbf{S}_x\mathbf{R}_x + 4\mathbf{I}_x\mathbf{S}_x\mathbf{R}_x$ . The full list of output states is given in Table 3.

It should be noted that, of the observable terms (i.e. those terms linear in  $\mathbf{I}_x$ ,  $\mathbf{S}_x$  and  $\mathbf{R}_x$ ), the term in  $\mathbf{R}_x$  always has the same phase, but the balanced functions have altered signs of  $\mathbf{I}_x$  or  $\mathbf{S}_x$ , or both. Thus if one observes that the  $\mathbf{I}_x$  or  $\mathbf{S}_x$  (or both) quartets are inverted one knows that the function is balanced.

We note however that the same goal can be achieved by starting with thermal rather than pure initial states. This is because, as we will show below, similar effects are observed from the outputs starting with thermal initial states as were visible starting from pure initial states. This is not the first time that it has been noted that in NMR quantum computers,

thermal initial states are sufficient to implement the algorithms of interest [6].

Thus in the NMR implementation that we will use, the theoretical steps [1] to [4] are replaced with

[1\*] **Preparation:** One starts with the thermal initial state

$$\mathbf{I}_z + \mathbf{S}_z + \mathbf{R}_z \quad (8)$$

[2\*] **Excitation:** Apply a hard  $\pi/2$  pulse along the  $y$ -axis to arrive at

$$\mathbf{I}_x + \mathbf{S}_x + \mathbf{R}_x \quad (9)$$

[3\*] **Evaluation:** Now evolve the system with one of the unitary operators given in Table 2. This is achieved by using simultaneous line selective pulses (see below).

For example under  $f_4$  the state evolves to

$$2\mathbf{I}_x\mathbf{R}_x + \mathbf{S}_x + \mathbf{R}_x. \quad (10)$$

The list of states to which each of  $\mathbf{I}_x$ ,  $\mathbf{S}_x$  and  $\mathbf{R}_x$  evolve is given in Table 4.

However (see below) the line selective pulses produce evolution by a unitary operator which is close to that required but differs by a controlled phase shift. For example, in the case of  $f_4$ , the line selective pulse produces the unitary transformation

$$\Delta(2i\sigma_x, 2i\sigma_x, E, E), \quad (11)$$

whereas the unitary given in Table 2 is

$$U_4 = \Delta(2\sigma_x, 2\sigma_x, E, E). \quad (12)$$

The relation between these two matrices is

$$U_4 = \Delta(2\sigma_x, 2\sigma_x, E, E) = \Delta(2i\sigma_x, 2i\sigma_x, E, E) \times \Delta(-iE, -iE, E, E). \quad (13)$$

The second matrix on the right hand side of this equation is a  $z$  rotation on the first spin by the angle  $\pi/2$ . Thus if one wants to implement  $U_4$ , it would be necessary to follow the line-selective pulse by a phase shift. One finds that similar phase shifts are required for all functions except  $f_1$  and  $f_2$ .

[4\*] **Observation:** Under evolution by the unitary operators corresponding to any of the balanced functions, either the  $I$  response or the  $S$  response (or both) disappears. Had we started with a pure initial state the equivalent line would have been inverted.

We note that the disappearance or otherwise of the  $I$  or  $S$  response is not affected by the final phase shift. This is because the state

$$\mathbf{I}_x + \mathbf{S}_x + \mathbf{R}_x \quad (14)$$

still evolves to states in which the same line disappears even if this last phase shift is not implemented. This may be appreciated by looking at the product operators to which the state evolves, as given in Table 5.

## 2 Experimental Realization

One possible way to implement the evaluation stage of the algorithm would be to make use of the fact [13] that any unitary transformation can be built up from combinations of the *controlled not* operation and operations on a single qubit. The implementation of a controlled not operation by magnetic resonance involves the preparation of nuclear magnetization vectors of a given spin aligned in opposite directions in the transverse plane. This “anti-phase” condition, which may be represented in the product operator formalism as (say)  $2\mathbf{I}_y\mathbf{S}_z$ , can be generated in a coupled two-spin system through the initial stages of the INEPT pulse sequence [14], relying on (refocused) evolution under the  $2\mathbf{I}_z\mathbf{S}_z$  operator for a fixed interval  $1/(2J_{IS})$ . However, the extension of this procedure to more than two coupled spins is complicated and not easy to implement. A more direct approach, and the one we have employed, is through the use of high-selectivity radio-frequency pulses designed to perturb transverse magnetization one line at a time. For example applying a  $\pi$  pulse with Hamiltonian of the form [15]

$$\mathbf{R}_x + 2\mathbf{I}_z\mathbf{R}_x + 2\mathbf{S}_z\mathbf{R}_x + 4\mathbf{I}_z\mathbf{S}_z\mathbf{R}_x \quad (15)$$

causes the system to evolve by the unitary operator

$$\Delta(2i\sigma_x, E, E, E). \quad (16)$$

The key observation from the point of view of our work is that more than one such line-selective perturbation may be applied simultaneously [16]. Thus any of the unitary

operators in Table 5 (and indeed a very wide class of controlled rotations about more general axes) may be produced in the same time that is required to produce the perturbation given in (16). It is worth noting that this time is of the same order as that required to implement the INEPT sequence. We feel that as well as being helpful for the present work, the method of manipulating spins via simultaneous line selective pulses may well prove advantageous in NMR quantum computers with more spins.

The experimental task is to shape the radio-frequency pulse envelope so as to achieve sufficient selectivity in the frequency domain that there is negligible perturbation of the next-nearest neighbour of the spin multiplet. In this sense the technique resembles that used in pseudo-two-dimensional spectroscopy [17] where the frequency of a soft radio-frequency pulse is stepped through the spectrum of interest in very small frequency increments, exciting the transitions one by one. We investigated several possible pulse shapes for this purpose, including rectangular, Gaussian, sine-bell, and triangular, before settling on the Gaussian as the most suitable for the task.

In a weakly-coupled three-spin *ISR* system the *R* spectrum is a doublet of doublets with splittings  $J_{IR}$  and  $J_{SR}$ . Application of  $\pi$  pulses to all four transverse *R*-spin magnetization components corresponds to a constant function in the sense of the Deutsch-Jozsa algorithm, and the “do nothing” experiment represents the other constant function. The balanced functions may be implemented by application of soft  $\pi$  pulses to the individual lines two at a time, for example  $[0, 0, \pi, \pi]$ ,  $[0, \pi, 0, \pi]$ , or  $[0, \pi, \pi, 0]$ , where 0 denotes no soft pulse. These cases, corresponding to functions  $f_3, f_6$  and  $f_8$  have Hamiltonians proportional to  $\mathbf{R}_x - 2\mathbf{I}_z\mathbf{R}_x$ ,  $\mathbf{R}_x - 2\mathbf{S}_z\mathbf{R}_x$  and  $\mathbf{R}_x - 4\mathbf{I}_z\mathbf{S}_z\mathbf{R}_x$  respectively. One way to calculate the effect of these Hamiltonians is to use standard product operator manipulations [15]. For example one finds that a  $\pi$  pulse with Hamiltonian of the form  $\mathbf{R}_x - 2\mathbf{I}_z\mathbf{R}_x$  leaves  $\mathbf{R}_x$  and  $\mathbf{S}_x$  unchanged and changes  $\mathbf{I}_x$  to  $2\mathbf{I}_y\mathbf{R}_x$  as in Table 5.

The practical implementation is deceptively simple. Starting with a thermal state, a hard  $\pi/2$  pulse about the *y* axis (denoted  $[\pi/2]_y$ ) excites transverse magnetizations  $\mathbf{I}_x$ ,  $\mathbf{S}_x$  and  $\mathbf{R}_x$ . The evaluation step is the application of line-selective  $[\pi]_x$  pulses to the individual components of the *R* multiplet. We may choose to apply soft  $[\pi]_x$  pulses to all four magnetization components, any two of the four, or none at all. In all cases the soft pulses are applied simultaneously, while the remaining transitions are simply left to evolve freely for the same period of time. However the perturbed magnetization components lose

intensity only through spin-spin relaxation during the relatively long interval of the soft pulse,  $T$ , because the effects of spatial inhomogeneity of the magnetic field are refocused, whereas the freely precessing components decay more rapidly, with a shorter time constant  $T_2^*$ . This difference in intensities serves to confirm which  $R$  transitions were perturbed.

Experiments were carried out at 400 MHz on a Varian VXR-400 spectrometer equipped with a waveform generator which controlled the shaped radiofrequency pulses. The three-spin proton system chosen for study was 2,3-dibromopropanoic acid in  $\text{CDCl}_3$ . The three coupling constants are  $J_{IR} = +11.3$  Hz,  $J_{IS} = -10.1$  Hz, and  $J_{RS} = +4.3$  Hz. (The negative sign of the geminal coupling  $J_{IS}$  [18] has no particular significance in these experiments.) Strong coupling effects are evident between spins  $I$  and  $S$ , with  $J_{IS}/\delta_{IS} = 0.12$ . Each soft  $[\pi]_x$  pulse can be thought of as acting on one of the four  $R$ -spin magnetizations in a rotating frame at the exact resonance frequency of that particular  $R$  line. These four reference frames rotate at four different frequencies  $(\pm J_{SR} \pm J_{IR})/2$  with respect to the transmitter frequency centred on the  $R$  chemical shift. The  $x$ -axes of all four frames must be coincident at the beginning of the soft pulse interval  $T$ . The duration of the soft pulse,  $T$ , may be chosen in such a way as to optimize the frequency selectivity.

The predicted result (Table 5), is to convert  $I$ - or  $S$ -spin magnetization into various forms of multiple-quantum coherence in the six cases where the  $R$  magnetization components are perturbed in pairs (the balanced functions) but to leave the  $I$ - and  $S$ -spin magnetizations unaffected in the remaining two cases where the four  $R$  magnetization components are all perturbed or all left alone (the constant functions). These predictions are clearly borne out by the experimental spectra shown in the Figure. In principle, complete conversion into unobservable multiple-quantum coherence would be detected by the disappearance of the appropriate  $I$  or  $S$ -spin response. In practice, owing to non-idealities of the system (for example strong coupling effects between  $I$  and  $S$ ) this is observed as a roughly eightfold loss of intensity rather than complete suppression.

Eight experiments were performed to test the eight cases of Table 5. The transmitter frequency was centred on the  $R$ -spin multiplet. Note that the  $R$  spectrum remains unperturbed throughout the series, except for the intensity perturbation mentioned above, a result of the refocusing effect of the soft  $\pi$  pulses. The phases of the  $I$ - and  $S$  signals will be determined by the scalar coupling and chemical shift evolution during the period

*T.* These complex phase patterns do not interfere with the Deutsch-Jozsa test because this involves only the observation of the “disappearance” of certain signals. These signal losses are made clearly evident by displaying absolute-value spectra, which may then be integrated. The integrated intensities are shown as percentages of the corresponding intensities in the top spectrum (no soft-pulse perturbation). Creation of multiple-quantum coherence is indicated by the roughly eightfold decrease in intensity in the appropriate places; all other *I*- and *S*-spin intensities remain essentially at 100%. This interpretation was confirmed in a second experiment with a multiplet-selective soft  $\pi/2$  pulse applied to the *R* spins at the end of the sequence. This has the effect of restoring the “lost” intensities by reconvertng *IR* and *SR* multiple-quantum coherence into observable magnetization.

Thus, in a single measurement, a distinction can be made between constant and balanced functions simply on the grounds of the “disappearance” of *I*- or *S*- spin lines. The fact that further details can be gleaned about the pattern of soft- pulse perturbation is irrelevant to the Deutsch-Jozsa algorithm. The extension to systems of more than three coupled spins is clear. Because the soft pulses are applied simultaneously, this involves no increase in the duration of the perturbation stage. The main limitation would be the magnitude of the smallest coupling constant, for this sets the frequency selectivity requirement. Extension to more qubits would most likely invoke the introduction of heteronuclear spins such as  $^{13}\text{C}$  and  $^{19}\text{F}$ .

**Acknowledgments** The authors are indebted to Dr Ēriks Kupĉe of Varian Associates for invaluable advice on the generation of shaped selective radio-frequency pulses.

## References

- [1] P. Shor, *Proc. 35<sup>th</sup> Ann. Symp. on Found. of Computer Science* (IEEE Comp. Soc. Press, Los Alamitos, CA, 1994) 124-134 .
- [2] D.G. Cory, A.F. Fahmy, and T.F. Havel, *Proc. Nat. Acad. Sci.* **94**, 1634 (1997).
- [3] D.G. Cory, M.D. Price, and T.F. Havel, LANL E-print quant-ph/9709001 (1997).
- [4] N. Gershenfeld, and I.L. Chuang, *Science* **275**, 350 (1997).
- [5] I.L. Chuang, N. Gershenfeld, M.G. Kubinec and D.W. Leung, *Proc. R. Soc. Lond., A*, **454**, 447 (1998).

- [6] I.L. Chuang, L.M.K. Vandersypen, X. Zhou, D.W. Leung and S. Lloyd, *Nature*, **393**, 143 (1998).
- [7] I.L. Chuang, N. Gershenfeld and M. Kubinec, *Phys. Rev. Lett.* **80**, 3408 (1998).
- [8] J.A. Jones, and M. Mosca, LANL E-print quant-ph/9801027 (1998).
- [9] J.A. Jones, M. Mosca, and R.H. Hansen, LANL E-print quant-ph/9805069 (1998).
- [10] D.G. Cory, W. Mass, M.D. Price, E. Knill, R. Laflamme, W.H. Zurek, T.F. Havel, and S.S. Somaroo, LANL E-print quant-ph/9802018 (1998).
- [11] D. Deutsch, and R. Jozsa, *Proc. R. Soc. Lond., A* **439**, 553 (1992).
- [12] L.K. Grover, *Phys. Rev. Lett.* **79**, 4709 (1997).
- [13] A. Barenco, C.H. Bennett, R. Cleve, D. P. DiVincenzo, N. Margolus, P. Shor, T. Sleator, J. Smolin, and H. Weinfurter, *Phys. Rev. A.* **52**, 3457 (1995).
- [14] G.A. Morris and R. Freeman, *J. Am. Chem. Soc.* **101**, 760 (1979).
- [15] O.W. Sorensen, G.W. Eich, M.H. Levitt, G. Bodenhausen, and R.R. Ernst, *Prog. NMR Spectroscopy*, **16**, 163 (1983).
- [16] Ě. Kupče, and R. Freeman, *J. Magn. Reson. A* **105**, 234 (1993).
- [17] S. Davies, J. Friedrich, and R. Freeman, *J. Magn. Reson.* **75**, 540 (1987).
- [18] R. Freeman, K.A. McLaughlan, J.I. Musher and K.G.R. Pachler, *Mol. Phys.* **5**, 321 (1962).

$x$	$f_1(x)$	$f_2(x)$	$f_3(x)$	$f_4(x)$	$f_5(x)$	$f_6(x)$	$f_7(x)$	$f_8(x)$
00	0	1	0	1	1	0	1	0
01	0	1	0	1	0	1	0	1
10	0	1	1	0	1	0	0	1
11	0	1	1	0	0	1	1	0

Table 1: The eight possible balanced or constant binary functions mapping two bits to one bit.

$f$	$U$
$f_1$	$\Delta(E, E, E, E)$
$f_2$	$\Delta(2\sigma_x, 2\sigma_x, 2\sigma_x, 2\sigma_x)$
$f_3$	$\Delta(E, E, 2\sigma_x, 2\sigma_x)$
$f_4$	$\Delta(2\sigma_x, 2\sigma_x, E, E)$
$f_5$	$\Delta(2\sigma_x, E, 2\sigma_x, E)$
$f_6$	$\Delta(E, 2\sigma_x, E, 2\sigma_x)$
$f_7$	$\Delta(2\sigma_x, E, E, 2\sigma_x)$
$f_8$	$\Delta(E, 2\sigma_x, 2\sigma_x, E)$

Table 2: The unitary operators corresponding to the eight constant or balanced binary functions mapping two bits to one bit.

$f$	output
$f_1$	$+\mathbf{I}_x + \mathbf{S}_x - \mathbf{R}_x + 2\mathbf{I}_x\mathbf{S}_x - 2\mathbf{I}_x\mathbf{R}_x - 2\mathbf{S}_x\mathbf{R}_x - 4\mathbf{I}_x\mathbf{S}_x\mathbf{R}_x$
$f_2$	$+\mathbf{I}_x + \mathbf{S}_x - \mathbf{R}_x + 2\mathbf{I}_x\mathbf{S}_x - 2\mathbf{I}_x\mathbf{R}_x - 2\mathbf{S}_x\mathbf{R}_x - 4\mathbf{I}_x\mathbf{S}_x\mathbf{R}_x$
$f_3$	$-\mathbf{I}_x + \mathbf{S}_x - \mathbf{R}_x - 2\mathbf{I}_x\mathbf{S}_x + 2\mathbf{I}_x\mathbf{R}_x - 2\mathbf{S}_x\mathbf{R}_x + 4\mathbf{I}_x\mathbf{S}_x\mathbf{R}_x$
$f_4$	$-\mathbf{I}_x + \mathbf{S}_x - \mathbf{R}_x - 2\mathbf{I}_x\mathbf{S}_x + 2\mathbf{I}_x\mathbf{R}_x - 2\mathbf{S}_x\mathbf{R}_x + 4\mathbf{I}_x\mathbf{S}_x\mathbf{R}_x$
$f_5$	$+\mathbf{I}_x - \mathbf{S}_x - \mathbf{R}_x - 2\mathbf{I}_x\mathbf{S}_x - 2\mathbf{I}_x\mathbf{R}_x + 2\mathbf{S}_x\mathbf{R}_x + 4\mathbf{I}_x\mathbf{S}_x\mathbf{R}_x$
$f_6$	$+\mathbf{I}_x - \mathbf{S}_x - \mathbf{R}_x - 2\mathbf{I}_x\mathbf{S}_x - 2\mathbf{I}_x\mathbf{R}_x + 2\mathbf{S}_x\mathbf{R}_x + 4\mathbf{I}_x\mathbf{S}_x\mathbf{R}_x$
$f_7$	$-\mathbf{I}_x - \mathbf{S}_x - \mathbf{R}_x + 2\mathbf{I}_x\mathbf{S}_x + 2\mathbf{I}_x\mathbf{R}_x + 2\mathbf{S}_x\mathbf{R}_x - 4\mathbf{I}_x\mathbf{S}_x\mathbf{R}_x$
$f_8$	$-\mathbf{I}_x - \mathbf{S}_x - \mathbf{R}_x + 2\mathbf{I}_x\mathbf{S}_x + 2\mathbf{I}_x\mathbf{R}_x + 2\mathbf{S}_x\mathbf{R}_x - 4\mathbf{I}_x\mathbf{S}_x\mathbf{R}_x$

Table 3: The output states from a (pseudo) pure initial state after the evaluation stage.

$f$	$U$	$\mathbf{I}_x$	$\mathbf{S}_x$	$\mathbf{R}_x$
$f_1$	$\Delta(E, E, E, E)$	$\mathbf{I}_x$	$\mathbf{S}_x$	$\mathbf{R}_x$
$f_2$	$\Delta(2\sigma_x, 2\sigma_x, 2\sigma_x, 2\sigma_x)$	$\mathbf{I}_x$	$\mathbf{S}_x$	$\mathbf{R}_x$
$f_3$	$\Delta(E, E, 2\sigma_x, 2\sigma_x)$	$2\mathbf{I}_x\mathbf{R}_x$	$\mathbf{S}_x$	$\mathbf{R}_x$
$f_4$	$\Delta(2\sigma_x, 2\sigma_x, E, E)$	$2\mathbf{I}_x\mathbf{R}_x$	$\mathbf{S}_x$	$\mathbf{R}_x$
$f_5$	$\Delta(2\sigma_x, E, 2\sigma_x, E)$	$\mathbf{I}_x$	$2\mathbf{S}_x\mathbf{R}_x$	$\mathbf{R}_x$
$f_6$	$\Delta(E, 2\sigma_x, E, 2\sigma_x)$	$\mathbf{I}_x$	$2\mathbf{S}_x\mathbf{R}_x$	$\mathbf{R}_x$
$f_7$	$\Delta(2\sigma_x, E, E, 2\sigma_x)$	$2\mathbf{I}_x\mathbf{R}_x$	$2\mathbf{S}_x\mathbf{R}_x$	$\mathbf{R}_x$
$f_8$	$\Delta(E, 2\sigma_x, 2\sigma_x, E)$	$2\mathbf{I}_x\mathbf{R}_x$	$2\mathbf{S}_x\mathbf{R}_x$	$\mathbf{R}_x$

Table 4: The effect on input product operators  $\mathbf{I}_x$ ,  $\mathbf{S}_x$  and  $\mathbf{R}_x$  of the unitary operators in the second column; for example under  $\Delta(E, 2\sigma_x, E, 2\sigma_x)$ , the input  $\mathbf{S}_x$  evolves to  $2\mathbf{S}_x\mathbf{R}_x$

$f$	$U$	$\mathbf{I}_x$	$\mathbf{S}_x$	$\mathbf{R}_x$
$f_1$	$\Delta(E, E, E, E)$	$\mathbf{I}_x$	$\mathbf{S}_x$	$\mathbf{R}_x$
$f_2$	$\Delta(2i\sigma_x, 2i\sigma_x, 2i\sigma_x, 2i\sigma_x)$	$\mathbf{I}_x$	$\mathbf{S}_x$	$\mathbf{R}_x$
$f_3$	$\Delta(E, E, 2i\sigma_x, 2i\sigma_x)$	$2\mathbf{I}_y\mathbf{R}_x$	$\mathbf{S}_x$	$\mathbf{R}_x$
$f_4$	$\Delta(2i\sigma_x, 2i\sigma_x, E, E)$	$-2\mathbf{I}_y\mathbf{R}_x$	$\mathbf{S}_x$	$\mathbf{R}_x$
$f_5$	$\Delta(2i\sigma_x, E, 2i\sigma_x, E)$	$\mathbf{I}_x$	$-2\mathbf{S}_y\mathbf{R}_x$	$\mathbf{R}_x$
$f_6$	$\Delta(E, 2i\sigma_x, E, 2i\sigma_x)$	$\mathbf{I}_x$	$2\mathbf{S}_y\mathbf{R}_x$	$\mathbf{R}_x$
$f_7$	$\Delta(2i\sigma_x, E, E, 2i\sigma_x)$	$-4\mathbf{I}_y\mathbf{S}_z\mathbf{R}_x$	$-4\mathbf{I}_z\mathbf{S}_y\mathbf{R}_x$	$\mathbf{R}_x$
$f_8$	$\Delta(E, 2i\sigma_x, 2i\sigma_x, E)$	$4\mathbf{I}_y\mathbf{S}_z\mathbf{R}_x$	$4\mathbf{I}_z\mathbf{S}_y\mathbf{R}_x$	$\mathbf{R}_x$

Table 5: The effect on input product operators  $\mathbf{I}_x$ ,  $\mathbf{S}_x$  and  $\mathbf{R}_x$  of the unitary operators in the second column; for example under  $\Delta(E, 2i\sigma_x, E, 2i\sigma_x)$ , the input  $\mathbf{S}_x$  evolves to  $2\mathbf{S}_y\mathbf{R}_x$ .

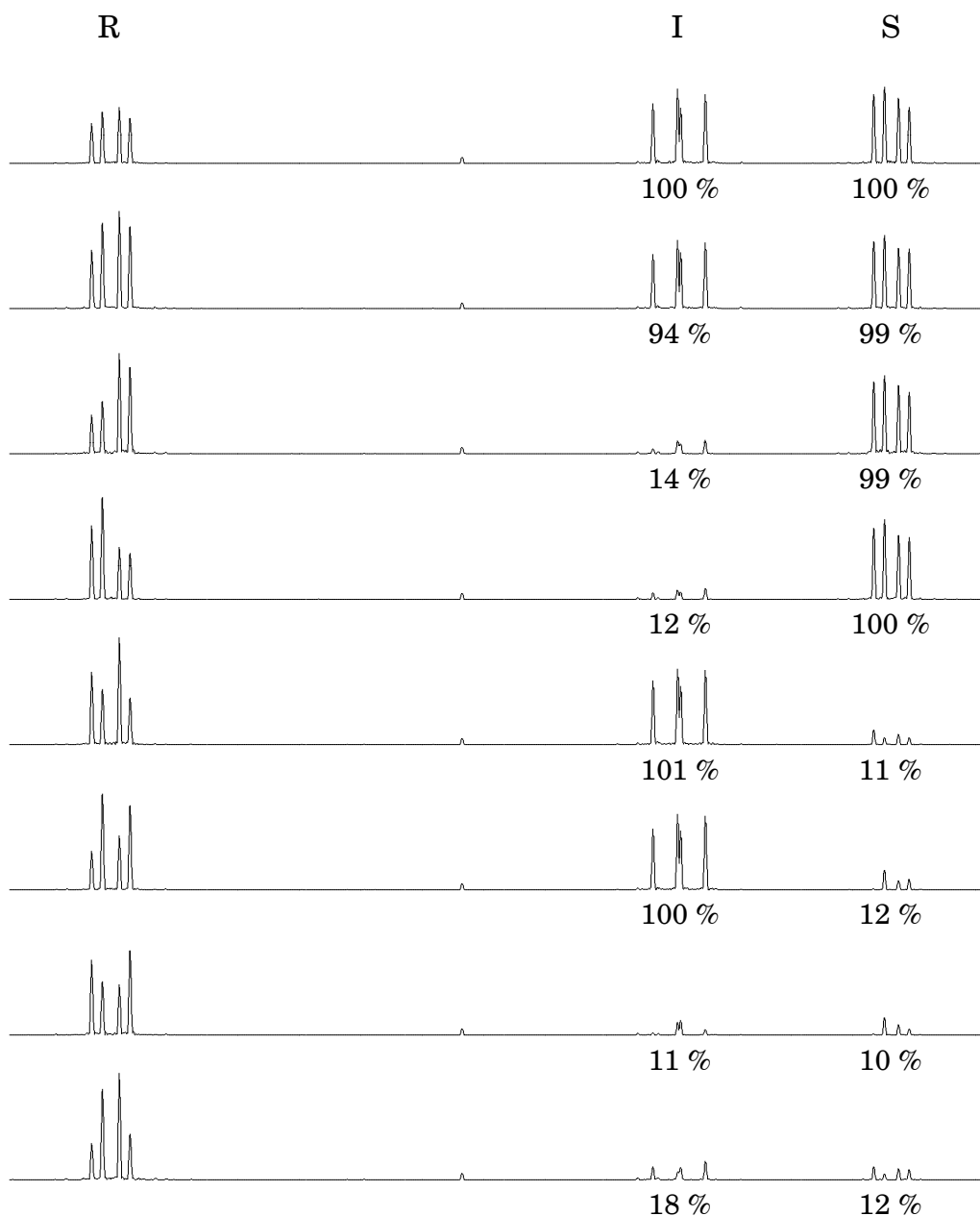


Figure 1: Eight absolute-value 400 MHz spectra of 2,3-dibromopropanoic acid obtained with the eight different perturbations set out in Table 5. The soft pulses were applied simultaneously with a pulse duration  $T = 0.65$  seconds. Reading from top to bottom, these spectra correspond to the functions  $f_1 \dots f_8$  of Table 1. Integrals of the  $I$ - and  $S$ -spin responses are shown as percentages of those in the top trace. After the evaluation of these integrals, the line shapes were improved by pseudo-echo weighting. Note the suppression of the appropriate  $I$ - and  $S$ -spin responses by about an order of magnitude.